

## LETTERS

## Climate change and the global malaria recession

Peter W. Gething<sup>1</sup>, David L. Smith<sup>2,3</sup>, Anand P. Patil<sup>1</sup>, Andrew J. Tatem<sup>2,4</sup>, Robert W. Snow<sup>5,6</sup> & Simon I. Hay<sup>1</sup>

The current and potential future impact of climate change on malaria is of major public health interest<sup>1,2</sup>. The proposed effects of rising global temperatures on the future spread and intensification of the disease<sup>3–5</sup>, and on existing malaria morbidity and mortality rates<sup>3</sup>, substantively influence global health policy<sup>6,7</sup>. The contemporary spatial limits of *Plasmodium falciparum* malaria and its endemicity within this range<sup>8</sup>, when compared with comparable historical maps, offer unique insights into the changing global epidemiology of malaria over the last century. It has long been known that the range of malaria has contracted through a century of economic development and disease control<sup>9</sup>. Here, for the first time, we quantify this contraction and the global decreases in malaria endemicity since approximately 1900. We compare the magnitude of these changes to the size of effects on malaria endemicity proposed under future climate scenarios and associated with widely used public health interventions. Our findings have two key and often ignored implications with respect to climate change and malaria. First, widespread claims that rising mean temperatures have already led to increases in worldwide malaria morbidity and mortality are largely at odds with observed decreasing global trends in both its endemicity and geographic extent. Second, the proposed future effects of rising temperatures on endemicity are at least one order of magnitude smaller than changes observed since about 1900 and up to two orders of magnitude smaller than those that can be achieved by the effective scale-up of key control measures. Predictions of an intensification of malaria in a warmer world, based on extrapolated empirical relationships or biological mechanisms, must be set against a context of a century of warming that has seen marked global declines in the disease and a substantial weakening of the global correlation between malaria endemicity and climate.

A resurgence in funding for malaria control<sup>10</sup>, the existing efficacy of affordable interventions, and a growing body of nationally or sub-nationally reported declines in endemicity or clinical burden<sup>11</sup> have engendered renewed optimism among the international malaria research and control community. In marked contrast, however, are model predictions, reported widely in global climate policy debates<sup>3,6,7</sup>, that climate change is adding to the present-day burden of malaria and will increase both the future range and intensity of the disease. In policy arenas, such predictions can support scenario analysis or serve as a call to action, but the modelling approaches used and the accuracy of their predictions have not always been challenged.

The recent publication of an evidence-based map of contemporary malaria endemicity<sup>8</sup> allows an audit of changes in the global epidemiology of malaria since the start of the twentieth century; a period of undoubted climatic change<sup>12</sup>. We compare this modern-day map with the most reliable equivalent for the pre-intervention era, around 1900 (ref. 13), and compare the magnitude of observed changes in range and endemicity to those proposed to occur in response to

climate change and observed under existing public health interventions. We use these perspectives to reassess the rationale of existing modelling approaches to impact assessments and the threat posed by future climatic changes to regional malaria control.

The only global map of pre-intervention malaria endemicity dates from a 1968 study<sup>13</sup> (Fig. 1a) in which a major synthesis of historical records, documents and maps of a variety of malariometric indices for all four *Plasmodium* species was used to map parasite rate (PR)—the

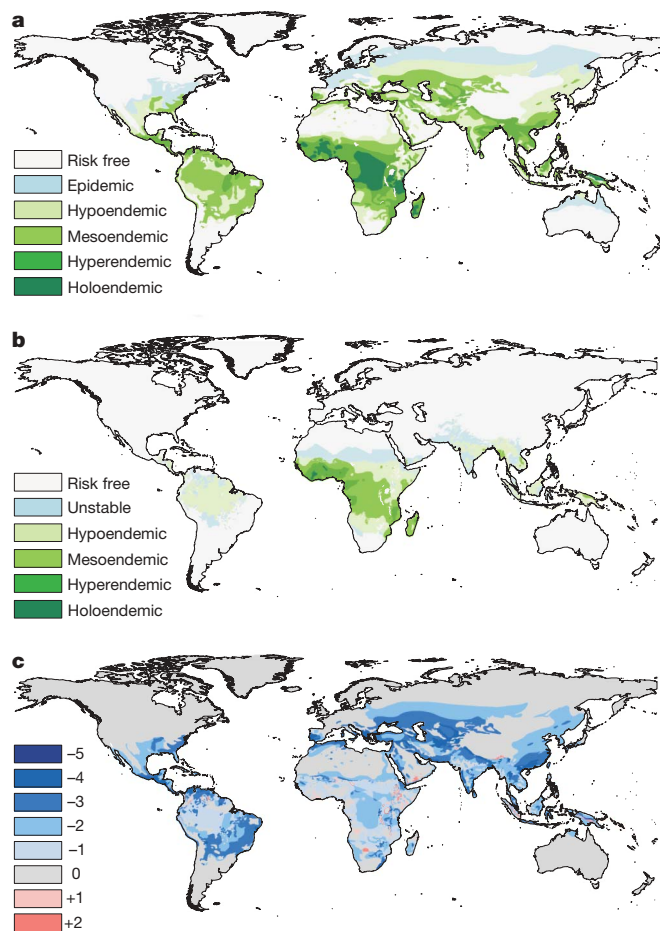


**Figure 1 | Changing global malaria endemicity since 1900.** **a**, Pre-intervention endemicity (approximately 1900) as defined in ref. 13. **b**, Contemporary endemicity for 2007 based on a recent global project to define the limits and intensity of current *P. falciparum* transmission<sup>8</sup>. **c**, Change in endemicity class between 1900 and 2007. Negative values denote a reduction in endemicity, positive values an increase.

<sup>1</sup>Spatial Ecology and Epidemiology Group, Tinbergen Building, Department of Zoology, University of Oxford, South Parks Road, Oxford OX1 3PS, UK. <sup>2</sup>Emerging Pathogens Institute, University of Florida, Gainesville, Florida 32610, USA. <sup>3</sup>Department of Biology, University of Florida, Gainesville, Florida 32610, USA. <sup>4</sup>Department of Geography, University of Florida, Gainesville, Florida 32611, USA. <sup>5</sup>Malaria Public Health and Epidemiology Group, Centre for Geographic Medicine, KEMRI – University of Oxford – Wellcome Trust Collaborative Programme, Kenyatta National Hospital Grounds (behind NASCOP), P.O. Box 43640-00100, Nairobi, Kenya. <sup>6</sup>Centre for Tropical Medicine, Nuffield Department of Clinical Medicine, University of Oxford, CCVTM, Oxford OX3 7LJ, UK.

proportion of individuals with malaria parasites in their peripheral blood) stratified into four endemic classes (hypoendemic,  $PR < 10\%$ ; mesoendemic,  $PR \geq 10\%$  and  $< 50\%$ ; hyperendemic,  $PR \geq 50\%$  and  $< 75\%$ ; holoendemic,  $PR \geq 75\%$ ). This map is the only reconstruction of historical malaria at its assumed historical peak around the start of the twentieth century and triangulates well with the plethora of national level malaria maps published throughout the last century (see ref. 14 for a systematic review).

We have used recently completed work that defines the 2007 limits of stable *P. falciparum* transmission and its endemicity within this range<sup>8</sup> to generate a comparable contemporary map of *P. falciparum* malaria distribution. This model has been described in detail elsewhere<sup>8</sup> and its output allowed for a continuous estimate of parasite prevalence for the year 2007 (Fig. 1b) stratified into the same endemicity classes used in the historical map<sup>13</sup> (see Methods). Comparison of the historical and contemporary maps revealed that endemic/stable malaria is likely to have covered 58% of the world's land surface around 1900 (see Supplementary Table 1) but only 30% by 2007 when *P. falciparum* malaria has become restricted largely to the tropics. Even more marked has been the decrease in prevalence within this greatly reduced range, with endemicity falling by one or more classes in over two-thirds (67%) of the current range of stable transmission (Fig. 1c). The contemporary map indicates that holoendemic *P. falciparum* malaria is now rare and limited to patches in West Africa totalling around 140,000 km<sup>2</sup>. The Americas are entirely hypoendemic for *P. falciparum*, as are very large sections of central and southeast Asia and substantial swathes of Africa.

When empirical relationships linking the current spatial distributions of surface temperature and malaria are extrapolated to predict future changes in disease range or intensity under scenarios of rising global temperatures, a necessary assumption is that all other factors either remain constant or have a relatively negligible effect. During a century in which global temperature increases have been unequivocal<sup>12,15</sup>, we have documented a marked, global decrease in the range and intensity of malaria transmission. This suggests that such an assumption would not have been valid for predicting the response of malaria to the warming climate of the last 100 years. A second assumption is that the nature of the link between climate and the global distribution and intensity of malaria is effectively immutable: an empirical climate–malaria relationship observed at one time period will be preserved even under changing climate and disease scenarios. However, a comparison of global-scale climate patterns with the historical and contemporary patterns of malaria endemicity presented here indicated a decoupling of the geographical climate–malaria relationship over the twentieth century (see Supplementary Information for additional explanation and results of this analysis), indicating that non-climatic factors have profoundly confounded this relationship over time. Contemporary endemicity maps therefore provide a poor baseline for empirically-based predictions of future climate effects.

Linking increasing temperatures to changes in malaria epidemiology is justified theoretically by known biological effects on different life-cycle stages of the *Anopheles* vector and *Plasmodium* parasite<sup>16</sup>. Such effects do not act in isolation, however, and empirical predictions are only credible if the role and relative influence of non-climatic factors is considered. A simple interpretation of the observed global recession in malaria since 1900 is that non-climatic factors, primarily direct disease control and the indirect effects of a century of urbanization and economic development, although spatially and temporally variable, have exerted a substantially greater influence on the geographic extent and intensity of malaria worldwide during the twentieth century than have climatic factors. This simple inference is consistent with other studies that have reviewed the historical climatic and anthropogenic forces acting on malaria<sup>17</sup> and has important implications for the debate on the importance of climate change in determining future malaria scenarios.

Biological modelling provides an alternative to empirical approaches, enabling the magnitude of potential disease responses to future climate scenarios to be estimated directly<sup>16,18,19</sup> and then

compared formally with observed or predicted effects from non-climatic influences. The *P. falciparum* basic reproductive number,  $PfR_0$ , quantifies the expected number of secondary cases in a non-immune population resulting from a single new infection and is the appropriate metric for comparing the relative magnitude of different effects on the underlying intensity of transmission<sup>20</sup>. Linked climate–biological models that simulate changes to  $PfR_0$  under different climate-change scenarios have proposed effect sizes of up to three (Table 1), that is, a tripling of the reproductive number<sup>16,18,19</sup>. To

**Table 1 | Comparison of magnitude of changes (effect size) in the basic reproductive number in relevant observational or predictive studies**

	Effect size (relative change in $R_0$ )	Study
<b>Estimated changes 1900–2007</b>		
Proportion of 1900 endemic world by area*		
13%	÷ ≤ 1†	This study
12%	÷ 1–10	This study
18%	÷ 10–100	This study
57%	÷ > 100	This study
<b>Changes predicted under climate change</b>		
Spatially aggregated mean change by ~2050‡§		
<i>P. falciparum</i>	× 1.27 (1.16–1.74)	Ref. 16
<i>P. vivax</i>	× 1.23 (1.15–1.39)	
Range of local changes by ~2050§¶	× 0–2	Ref. 16
Range of local changes by ~2080§¶	× 0–2#	Ref. 19
Range of local changes by ~2050§¶	× 0–3	Ref. 18
<b>Example effect sizes for interventions predicted via biological modelling</b>		
ACTs (compared to failing pre-ACT treatment)	÷ 1.1–1.8☆	Ref. 21
ITNs (at 40–60% effective coverage)	÷ 5–15**	Ref. 22
ITNs + LCI (both at 'moderate' coverage levels)	÷ 15–25††	Ref. 23
<b>Example effect sizes observed concurrently with increased intervention coverage (primary interventions in use)</b>		
Western Kenya‡‡ (ITNs, ITNs + LCI)	÷ 7.2††, ÷ 26.4††	Ref. 25
São Tomé and Príncipe§§ (IRS + ITNs + ACT + IPTp)	÷ 5.1	Ref. 26
Bioko Island¶¶ (IRS + ACT)	÷ 2.9##	Ref. 27
Southern Mozambique☆☆ (IRS + ACT)	÷ 78.8***	Ref. 28
Zanzibar††† (ITNs + ACT); 0–5 yr, 6–14 yr	÷ 1.6‡‡‡, ÷ 1.8‡‡‡	Ref. 29

ACT, Artemisinin-based combination therapy; EIR, entomological inoculation rate; IPTp, intermittent preventive treatment in pregnancy; ITN, insecticide-treated bed net; LCI, larval control intervention.

\* Percentages do not sum to 100 because of rounding. † Consists of 11% of land area with no evidence of change, and 2% with evidence of increased transmission. ‡ The available results relate to the combined Africa, South-East Asia, and Central and South America regions. Given are central modelled values and uncertainty intervals associated with plausible ranges of input biological parameters. § Results obtained using the MIASMA linked climate-biological model, under three future climate scenarios, and only the largest predicted changes are shown here. ¶ In the original study, results were not presented for areas with very low baseline potential to avoid using infinitesimal values as denominators in the comparison. ¶ Results apply to both *P. falciparum* and *P. vivax*. # Range of predicted changes included a '>2' category but no further details provided. ☆ Study reported predicted changes in parasite rate from five real-world baseline endemicity settings under failing treatment regimes based on pre-ACT monotherapies (Table 4 in ref. 21). We converted transitions in parasite rate into transitions in  $R_0$  to estimate effect size. \*\* Study modelled effect size as a continuous function of ITN effective coverage. Values presented based on Fig. 1 in ref. 22. †† Study reported effect sizes in terms of EIR, which were interpreted directly as  $R_0$  effect sizes. ‡‡ Results from a control trial. §§ Integrated malaria control effort involving mass intervention coverage complemented with health system strengthening. Reported decline relates to period 2005–2007. ||| Study reported reduction in community parasite rate from 30.5% to 2.1% following expanded control efforts. We converted this into transitions in  $R_0$  to estimate effect size. ¶¶ Integrated malaria control effort involving mass IRS administration, improved case management with ACT and strengthened health system surveillance and diagnostics. Reported decline relates to period 2004–2005. ## Study reported reduction in community parasite rate from 46% to 31% following expanded control efforts. We converted this into transitions in  $R_0$  to estimate effect size. ☆☆ Integrated malaria control effort involving IRS administration, improved case management with ACT and strengthened health systems. Reported decline relates to period 1999–2005. \*\*\* Study reported reduction in community parasite rate from 65% to 4% in study zone with longest running intervention coverage (Zone 1, values taken from Table 1 of ref. 28). We converted this into transitions in  $R_0$  to estimate effect size. ††† Integrated malaria control effort involving scale up of long-lasting ITNs from 10% to 90% coverage of children, switch from chloroquine to ACT as first and second line therapeutic and strengthened surveillance and health systems. Reported decline relates to period 2003–2005. ‡‡‡ Study reported reduction in parasite rate in children 0–5 yr from 9% to 0.3% and in children 6–14 yr from 12.9% to 1.7% following expanded control efforts. We converted this into transitions in  $R_0$  to estimate effect size.

place the proposed magnitude of these effects in context, we compared them to the observed reductions in global endemicity over the past century. To allow such a comparison, a simple *P. falciparum* transmission model<sup>20</sup> was used to translate the historic and contemporary estimated endemicity classes into approximate values of the reproductive number (see Methods). Using this model, the hypoendemic class (central PR value = 5%) was interpreted as representing an approximate  $R_0$  value of 1.3; holoendemic (central PR = 30%) as 5.5; mesoendemic (central PR = 63%) as 87.7; and hyperendemic (central PR = 88%) as 175.6. These conversions allowed the observed changes between historical and contemporary endemicity to be recast in terms of proportional changes (effect sizes) in the reproductive number and summarized simply into orders of magnitude to reflect their likely precision. In this way we found that, of the 66 million km<sup>2</sup> of the Earth's surface thought to have sustained stable/endemic malaria in 1900, 12%, 18% and 57% had exhibited proportional decreases in the reproductive number of up to one, between one and two, and greater than two orders of magnitude, respectively; 11% had shown no evidence of change; and 2% had shown evidence of an increase in the reproductive number by 2007 (see Supplementary Information for additional details of methods and results). Although imperfect, this simple comparison illustrates that despite warming global temperatures<sup>12</sup>, the combined natural and anthropogenic forces acting on the disease throughout the twentieth century have resulted in the great majority of locations undergoing a net reduction in transmission between one and three orders of magnitude larger than the maximum future increases proposed under temperature-based climate change scenarios (Table 1).

If the effects of climate change are to reverse the observed declining trend in malaria endemicity, they must exceed the collective counteracting effects of continuing economic development and increasing control efforts. Whereas the former is hard to quantify, the potency of currently available control and intervention tools has been assessed theoretically using biological models<sup>21–23</sup> and also evaluated in practice when changes in local transmission have been measured concurrently with aggressive malaria control initiatives<sup>24–29</sup>. We translated examples of predicted and observed changes in endemicity caused by control efforts into  $PfR_0$  effect sizes and compared these directly with effect sizes proposed under climate change. This indicated that suites of interventions at high coverage can achieve effect sizes exceeding two orders of magnitude (Table 1). When compared to the substantially smaller proposed magnitude of climate-induced effects, an important and simple inference is that the latter can be offset by moderate increases in coverage levels of currently available interventions.

Various sources of uncertainty exist in the inputs and methodologies used in this study. The proposed levels of historical endemicity<sup>13</sup> are plausible when triangulated against other values reported from the pre-intervention era (for example, see refs 28, 30 and 31), but the relatively crude categorization of all-cause malaria endemicity strata and the cartographic approach used preclude a more formal quantification of the precision in the global *P. falciparum* endemicity declines we report, and the subsequent conversions into *P. falciparum* reproductive number effect sizes are approximate. However, the key comparisons we present between observed declines, proposed temperature-driven increases, and the impact of available countermeasures rely on our estimates being accurate only to within one order of magnitude. We have compared two snapshots of estimated global endemicity separated by a period of 100 years during which changes in global temperatures have been accelerating, with the largest observed warming occurring in recent decades<sup>12</sup>. The progression of the recession in global malaria is less well measured, and several periods of decline and resurgence are known to have occurred associated with, for example, periods of coordinated large-scale control efforts, the introduction and subsequent failure of successive therapeutics, or breakdowns in public health infrastructure associated with conflict or political upheaval. There is, however, no evidence of a systematic upturn in malaria endemicity concurrent with the warming trend of

recent decades, while a growing body of evidence points to recent regional declines in malaria morbidity or mortality in areas achieving sustained intervention coverage<sup>11,26–29</sup>. We have interpreted the results presented in this study at a global scale. Any effects of rising temperatures on malaria transmission would most likely be extremely geographically variable, with most modelling studies suggesting that the fringes of the current disease extent would be most sensitive to warming<sup>5,16,19</sup>. However, these more local predictions are themselves largely undermined by current observations; the marginal transmission zones are the places from which the largest declines in malaria transmission or morbidity are being reported, concurrent with improved intervention coverage<sup>26–29</sup> and consistent with biological modelling studies that indicate a greater theoretical impact on endemicity in areas of lower baseline transmission<sup>32</sup>.

In an era when the international community has been emboldened to provide guidelines for malaria elimination it is necessary to maintain the correct perspective on the future impact of climate change on malaria epidemiology and by implication its malaria public health importance. The quantification of a global recession in the range and intensity of malaria over the twentieth century has allowed us to review the rationale underpinning high-profile predictions of a current and future worsening of the disease in a warming climate. It suggests that the success or failure of our efforts against the parasite in the coming century are likely to be determined by factors other than climate change.

## METHODS SUMMARY

The historical malaria endemicity map<sup>13</sup> was scanned from the original publication, digitized on-screen and rasterized to a 5 × 5 km grid. The map of contemporary malaria endemicity was generated from a recently defined model<sup>8</sup> of age-standardised *P. falciparum* parasite rate,  $PfPR_{2-10}$ . Using a model-based geostatistical framework, the underlying value of  $PfPR_{2-10}$  at each location was modelled for the year 2007 as a transformation of a space-time Gaussian process (GP), with the number of *P. falciparum*-positive individuals in each survey modelled as a binomial variate given the unobserved age-standardised prevalence surface. The GP was parameterised by a mean component (a linear function of time and urban–peri-urban–rural status) and a space-time covariance function which was spatially anisotropic, used great-circle distance to incorporate the curvature of the earth, and included a periodic temporal component to capture seasonality. Bayesian inference was implemented using Markov chain Monte Carlo and direct simulation to generate posterior predictive samples of the 2007 annual mean prevalence surface and to assign each pixel to the endemicity class with the highest posterior probability of membership.

Predicted  $PfPR_{2-10}$  values at each pixel were converted into approximate values of the *P. falciparum* basic reproductive number,  $PfR_0$ , using a model that assumes new infections are acquired and clear independently at a constant rate and that biting is heterogeneously distributed in a population such that relative biting rates follow a Gamma distribution.  $PfPR$  was empirically related to the  $PfEIR$  using a log-linear relationship based on 91 paired observations.  $PfEIR$  can be inferred from  $PfPR(X)$  by inverting the formula<sup>20,22</sup>. It follows that:

$$R_0 = \frac{|((1-X)^{-\alpha} - 1)|}{\alpha} \frac{c(1+S\kappa)(1+\alpha)}{\kappa}$$

where  $\kappa$  is the net infectiousness of humans, that is, the probability that a mosquito will become infected after biting a human,  $c$  is the probability that a mosquito will become infected after biting a non-immune infectious human, and  $S$  is the stability index.

**Full Methods** and any associated references are available in the online version of the paper at [www.nature.com/nature](http://www.nature.com/nature).

Received 3 February; accepted 16 April 2010.

1. Patz, J. A., Campbell-Lendrum, D., Holloway, T. & Foley, J. A. Impact of regional climate change on human health. *Nature* **438**, 310–317 (2005).
2. Lafferty, K. D. The ecology of climate change and infectious diseases. *Ecology* **90**, 888–900 (2009).
3. McMichael, A. J. et al. in *Comparative Quantification of Health Risks: Global and Regional Burden of Disease due to Selected Major Risk Factors* (eds Ezzati, M., Lopez, A. D., Rodgers, A. & Murray, C. J. L.) 1543–1649 (World Health Organization, 2004).
4. Tanser, F. C., Sharp, B. & Le Sueur, D. Potential effect of climate change on malaria transmission in Africa. *Lancet* **362**, 1792–1798 (2003).



5. van Lieshout, M., Kovats, R. S., Livermore, M. T. J. & Martens, P. Climate change and malaria: analysis of the SRES climate and socio-economic scenarios. *Glob. Environ. Change* **14**, 87–99 (2004).
6. Intergovernmental Panel on Climate Change. *Climate Change 2007: Impacts, Adaptation and Vulnerability. Contribution of Working Group II to the Fourth Assessment Report of the Intergovernmental Panel on Climate Change* (eds Parry, M. L., Canziani, O. F., Palutikof, J. P., van der Linden, P. J. & Hanson, C. E.) (Cambridge Univ. Press, 2007).
7. US Environmental Protection Agency. *Endangerment and Cause or Contribute Findings for Greenhouse Gases Under Section 202(a) of the Clean Air Act (Technical Support Document)* (US Environmental Protection Agency, 2010).
8. Hay, S. I. et al. A world malaria map: *Plasmodium falciparum* endemicity in 2007. *PLoS Med.* **6**, e1000048 (2009).
9. Hay, S. I., Guerra, C. A., Tatem, A. J., Noor, A. M. & Snow, R. W. The global distribution and population at risk of malaria: past, present, and future. *Lancet Infect. Dis.* **4**, 327–336 (2004).
10. Snow, R. W., Guerra, C. A., Mutheu, J. J. & Hay, S. I. International funding for malaria control in relation to populations at risk of stable *Plasmodium falciparum* transmission. *PLoS Med.* **5**, e142 (2008).
11. World Health Organization. *World malaria report 2009* (World Health Organization, 2009).
12. Intergovernmental Panel on Climate Change. *Climate Change 2007: The Physical Science Basis. Contribution of Working Group I to the Fourth Assessment Report of the Intergovernmental Panel on Climate Change* (eds Solomon, S. et al.) (Cambridge Univ. Press, 2007).
13. Lysenko, A. J. & Semashko, I. N. [in Russian] in *Itogi Nauki: Medicinskaja Geografija* (ed. Lebedew, A. W.) 25–146 (Academy of Sciences, Moscow, 1968).
14. Mouchet, J. et al. *Biodiversité du paludisme dans le monde* [in French] (John Libbey Eurotext, 2004).
15. Small, J., Goetz, S. J. & Hay, S. I. Climatic suitability for malaria transmission in Africa, 1911–1995. *Proc. Natl Acad. Sci. USA* **100**, 15341–15345 (2003).
16. Martens, W. J. M., Jetten, T. H. & Focks, D. A. Sensitivity of malaria, schistosomiasis and dengue to global warming. *Clim. Change* **35**, 145–156 (1997).
17. Reiter, P. Global warming and malaria: knowing the horse before hitching the cart. *Malaria J.* **7** (Suppl. 1), S3 (2008).
18. Lindsay, S. W. & Martens, W. J. M. Malaria in the African highlands: past, present and future. *Bull. World Health Organ.* **76**, 33–45 (1998).
19. Martens, P. et al. Climate change and future populations at risk of malaria. *Glob. Environ. Change* **9**, S89–S107 (1999).
20. Smith, D. L., McKenzie, F. E., Snow, R. W. & Hay, S. I. Revisiting the basic reproductive number for malaria and its implications for malaria control. *PLoS Biol.* **5**, e42 (2007).
21. Okell, L. C., Drakeley, C. J., Bousema, T., Whitty, C. J. & Ghani, A. C. Modelling the impact of artemisinin combination therapy and long-acting treatments on malaria transmission intensity. *PLoS Med.* **5**, e226 (2008).
22. Smith, D. L., Hay, S. I., Noor, A. M. & Snow, R. W. Predicting changing malaria risk after expanded insecticide-treated net coverage in Africa. *Trends Parasitol.* **25**, 511–516 (2009).
23. Killeen, G. F. et al. The potential impact of integrated malaria transmission control on entomologic inoculation rate in highly endemic areas. *Am. J. Trop. Med. Hyg.* **62**, 545–551 (2000).
24. Kouznetsov, R. L. Malaria control by application of indoor spraying of residual insecticides in tropical Africa and its impact on community health. *Trop. Doct.* **7**, 81–91 (1977).
25. Fillinger, U., Ndenga, B., Githeko, A. & Lindsay, S. W. Integrated malaria vector control with microbial larvicides and insecticide-treated nets in western Kenya: a controlled trial. *Bull. World Health Organ.* **87**, 655–665 (2009).
26. Teklehaimanot, H. D., Teklehaimanot, A., Kiszewski, A., Rampao, H. S. & Sachs, J. D. Malaria in São Tomé and Príncipe: on the brink of elimination after three years of effective antimalarial measures. *Am. J. Trop. Med. Hyg.* **80**, 133–140 (2009).
27. Kleinschmidt, I. et al. Reduction in infection with *Plasmodium falciparum* one year after the introduction of malaria control interventions on Bioko Island, Equatorial Guinea. *Am. J. Trop. Med. Hyg.* **74**, 972–978 (2006).
28. Sharp, B. L. et al. Seven years of regional malaria control collaboration - Mozambique, South Africa, and Swaziland. *Am. J. Trop. Med. Hyg.* **76**, 42–47 (2007).
29. Bhattarai, A. et al. Impact of artemisinin-based combination therapy and insecticide-treated nets on malaria burden in Zanzibar. *PLoS Med.* **4**, e309 (2007).
30. Smith, D. L., Dushoff, J., Snow, R. W. & Hay, S. I. The entomological inoculation rate and *Plasmodium falciparum* infection in African children. *Nature* **438**, 492–495 (2005).
31. Smith, D. L., Guerra, C. A., Snow, R. W. & Hay, S. I. Standardizing estimates of the *Plasmodium falciparum* parasite rate. *Malar. J.* **6**, 131 (2007).
32. Smith, D. L. & Hay, S. I. Endemicity response timelines for *Plasmodium falciparum* elimination. *Malar. J.* **8**, 87 (2009).

**Supplementary Information** is linked to the online version of the paper at [www.nature.com/nature](http://www.nature.com/nature).

**Acknowledgements** We thank A. Bibby, H. C. J. Godfray, G. D. Shanks and G. R. W. Wint for comments on the manuscript. S.I.H. is funded by a Senior Research Fellowship from the Wellcome Trust (#079091) that also supports P.W.G. and previously A.J.T. R.W.S. is funded by a Principal Research Fellowship from the Wellcome Trust (#079080) that also supports A.P.P. D.L.S. and A.J.T. are supported by a grant from the Bill and Melinda Gates Foundation (#49446). D.L.S. and S.I.H. also acknowledge funding support from the RAPIDD program of the Science & Technology Directorate, Department of Homeland Security, and the Fogarty International Center, National Institutes of Health. This work forms part of the output of the Malaria Atlas Project (MAP, <http://www.map.ox.ac.uk>), principally funded by the Wellcome Trust, UK.

**Author Contributions** S.I.H. conceived the research. P.W.G. and S.I.H. drafted the manuscript. P.W.G. led, and A.P.P., D.L.S., A.J.T. and R.W.S. contributed to, the analyses. All authors discussed the results and contributed to the revision of the final manuscript.

**Author Information** Reprints and permissions information is available at [www.nature.com/reprints](http://www.nature.com/reprints). The authors declare no competing financial interests. Readers are welcome to comment on the online version of this article at [www.nature.com/nature](http://www.nature.com/nature). Correspondence and requests for materials should be addressed to S.I.H. ([simon.hay@zoo.ox.ac.uk](mailto:simon.hay@zoo.ox.ac.uk)) or P.W.G. ([peter.getting@zoo.ox.ac.uk](mailto:peter.getting@zoo.ox.ac.uk)).

## METHODS

**Generating comparable historical and contemporary endemicity maps.** The historical malaria endemicity map<sup>13</sup> was scanned from the original publication and geo-referenced using ERDAS Imagine 8.5 (Leica Geosystems GIS & Mapping). The map was then digitised on-screen with MapInfo Professional 7.0 (MapInfo), and rasterized to a  $5 \times 5$  km grid. The map of contemporary malaria endemicity was generated from a recently defined model<sup>8</sup> of *P. falciparum* infection prevalence within the previously defined limits of stable transmission<sup>33</sup>. The underlying value of *P. falciparum* parasite rate in the 2–10-year age cohort,  $PfPR_{2-10}(x_i)$ , at each location  $x_i$  was modelled for the year 2007 as a transformation  $g(\cdot)$  of a space-time Gaussian process  $f(x_i, t_i)$  with mean  $\mu$  and covariance  $C$  superimposed with additional aspatial (random) variation  $\epsilon(x_i)$ , represented as Gaussian with zero mean and variance  $V$ . The number of *P. falciparum* positive individuals,  $N_i^+$ , from the total sample of  $N_i$  in each survey was modelled as a conditionally independent binomial variate given the unobserved underlying age-standardized  $PfPR_{2-10}$  value<sup>34</sup>. The space-time mean component  $\mu$  was modelled as a linear function of time,  $t$ , and urban–peri-urban–rural status (denoted by the indicator variables  $1_{u1}(x)$ ,  $1_{p1}(x)$ ). The mean component was therefore defined as:

$$\mu = \beta_x + \beta_t t + \beta_{u1} 1_{u1}(x) + \beta_{p1} 1_{p1}(x)$$

where  $\beta_x$  denotes the intercept. Each parasite rate survey was referenced temporally using the mid-point (in decimal years) between the recorded start and end months. Covariance between spatial and temporal locations was modelled using a spatially anisotropic space-time covariance function  $C$  with a periodic component (wavelength = 12 months) added to the time-marginal covariance model to capture seasonality<sup>35</sup>:

$$C(x_i, t_i; x_j, t_j) = \tau^2 \gamma(0) \frac{(\Delta x)^{\gamma(\Delta t)} K_{\gamma(\Delta t)}(\Delta x)}{2^{\gamma(\Delta t)-1} \Gamma(\gamma(\Delta t) + 1)},$$

$$\gamma(\Delta t) = \frac{1}{2\rho + 2(1-\rho)[(1-v)e^{-|\Delta t|/\phi} + v \cos(2\pi\Delta t)]},$$

$$\Delta t = |t_i - t_j|$$

where  $K_{\gamma}$  is the modified Bessel function of the second kind of order  $\gamma$ , and  $\Gamma$  is the gamma function<sup>36,37</sup>. The effect of the curvature of the earth on point-to-point separations, and a mechanism for spatial anisotropy, were incorporated by computing the spatial distance between a pair of points  $x_i$  and  $x_j$  as great-circle distance  $D_{GC}(x_i, x_j)$  on a flexible ellipsoid. Bayesian inference was implemented using Markov Chain Monte Carlo to generate samples from the posterior distribution of the Gaussian field  $f(x_i, t_i)$  at each data location and of the unobserved parameters of the mean, covariance function and Gaussian random noise component and direct simulation was then used to generate samples from the 2007 annual mean of the posterior distribution of  $f(x_i, t_i)$  at each prediction location across the same template  $5 \times 5$  km grid as that used for the historical map. Model output therefore consisted of samples from the posterior predictive distribution of the 2007 annual mean  $PfPR_{2-10}$  at each grid location. We assigned each pixel to the historical

endemicity class with the highest posterior probability of membership, identified as the class containing the largest proportion of posterior samples. Pixels modelled as being at unstable or no risk were assigned directly because these classifications were deterministic. The age-standardization (2–10-year-olds) matched that used in the historical map<sup>13</sup> except for the holoendemic class ( $PfPR > 70\%$ ) which the authors defined as relating to prevalence in one-year-olds.

**Translating predicted endemicity into approximate values of  $PfR_0$ .** We have developed a function to estimate the  $PfR_0$  from the  $PfPR$  on the basis of a model that assumes that new infections are acquired and clear independently at a constant rate and that biting is heterogeneously distributed in a population such that relative biting rates follow a Gamma distribution with mean 1 and variance  $\alpha^{20,22,30}$ . The transformation was developed with 91 paired estimates of the  $PfEIR$  and the  $PfPR$  in African children, standardized following an algorithm described in ref. 31.  $PfPR$  is empirically related to the  $PfEIR$  in these 91 paired estimates by a log-linear relationship<sup>38</sup>, or by a simple formula that describes the steady state of a malaria transmission model<sup>20</sup>.  $PfEIR$  can be inferred from  $PfPR(X)$  by inverting the formula<sup>20,22</sup>. It follows that:

$$R_0 = \frac{|((1-X)^{-\alpha} - 1)|}{\alpha} \frac{c(1+S\kappa)(1+\alpha)}{\kappa}$$

where  $\kappa$  is the net infectiousness of humans, the probability that a mosquito will become infected after biting a human,  $c$  is the probability that a mosquito will become infected after biting a non-immune infectious human, and  $S$  is the stability index.

The transformation from  $PfPR$  to  $PfEIR$  gives unsatisfactory estimates of  $PfEIR$  when  $PfPR$  exceeds approximately 65%. At these high values of  $PfEIR$  and  $PfPR$ , it is generally possible to find a value such that the function fits exactly. These values are statistically significantly and negatively correlated with  $PfPR$ , by the relationship  $\alpha = 9.292 - 8.035X$ . To make the transformation, we take  $\alpha = \min(4.2, 9.292 - 8.035X)$ . To make the transformation from  $PfPR$  to net infectiousness, we assume  $c = 0.1$  consistent with ref. 39, and we use the formula described elsewhere<sup>20,22</sup>, assuming no immunity. We also assume that  $S = 1$ , although  $\kappa < 1$ , and  $S$  is generally lower than approximately 5, so  $1 < 1 + S\kappa < 1.5$ .

33. Guerra, C. A. *et al.* The limits and intensity of *Plasmodium falciparum* transmission: implications for malaria control and elimination worldwide. *PLoS Med.* **5**, e38 (2008).
34. Diggle, P. & Ribeiro, P. J. *Model-based Geostatistics* (Springer, 2007).
35. Stein, M. L. Space-time covariance functions. *J. Am. Stat. Assoc.* **100**, 310–321 (2005).
36. Antosiewicz, H. A. in *Handbook of Mathematical Functions* (eds Abramowitz, M. & Stegun, I. A.) 435–479 (Dover Publications, 1964).
37. Davis, G. M. in *Handbook of Mathematical Function* (eds Abramowitz, M. & Stegun, I. A.) 253–295 (Dover Publications, 1964).
38. Hay, S. I., Guerra, C. A., Tatem, A. J., Atkinson, P. M. & Snow, R. W. Urbanization, malaria transmission and disease burden in Africa. *Nature Rev. Microbiol.* **3**, 81–90 (2005).
39. Killeen, G. F., Ross, A. & Smith, T. Infectiousness of malaria-endemic human populations to vectors. *Am. J. Trop. Med. Hyg.* **75**, 38–45 (2006).